Bioorganic & Medicinal Chemistry Letters 20 (2010) 4725–4737

Contents lists available at ScienceDirect

Bioorganic & Medicinal Chemistry Letters

journal homepage: www.elsevier.com/locate/bmcl

Bioorganic & Medicinal Chemistry Letters Volume 20, Issue 16, 2010

Contents

BMCL DIGEST

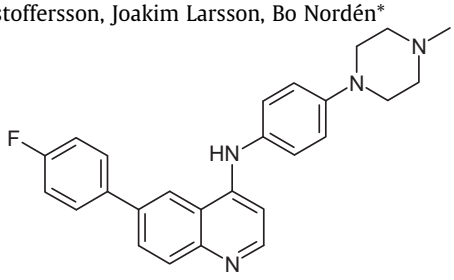

2g

Compound **2g** was found effective in reducing LPS-induced TNFα production in THP-1 cells, in a manner consistent with MK2 enzyme inhibition.

REGULAR ARTICLES

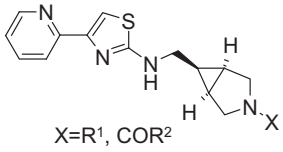

The synthesis and SAR of a series of potent NPY Y5 antagonists (fpKi >9) is reported.

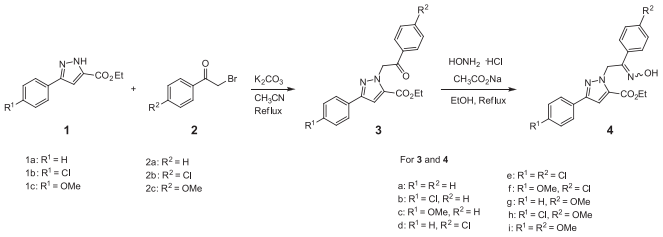

A series of novel oxime-containing pyrazole derivatives were synthesized and characterized by IR, ^{1}H NMR, HRMS spectroscopy, and X-ray analysis. A dose- and time-dependent inhibition of proliferation was observed in A549 lung cancer cell after compounds treatment. Hoechst 33258 staining assay and Western blot analysis of LC3-II level showed that the inhibition against A549 cell growth might be attributed to apoptosis and autophagy.

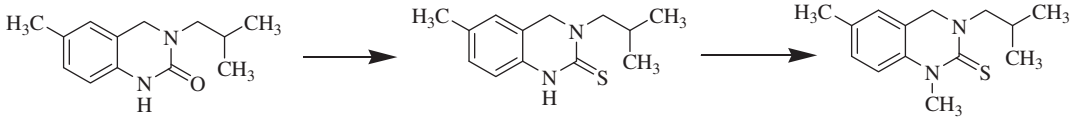

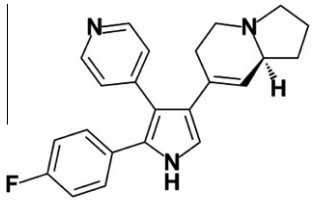

4a (R-132811)

We found that the most promising compound **4a** (R-132811) in this series inhibits the production of the proinflammatory cytokines in vitro and in vivo (e.g., TNFα IC_{50} = 0.026 μM, TNFα ID_{50} = 0.93 mg/kg).

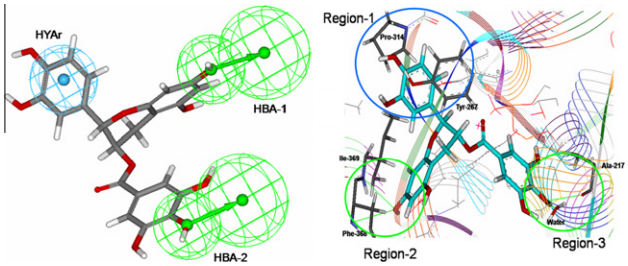

A common feature pharmacophore with two hydrogen-bond acceptor and one aromatic hydrophobic feature has been generated using seven active flavonoids. Docking studies of these compounds well corroborates with the pharmacophore model. Therefore model could be useful for identification of potential novel FAS-II inhibitors.

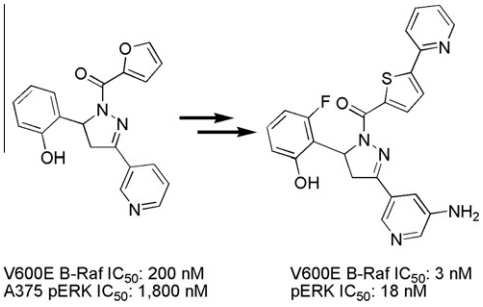

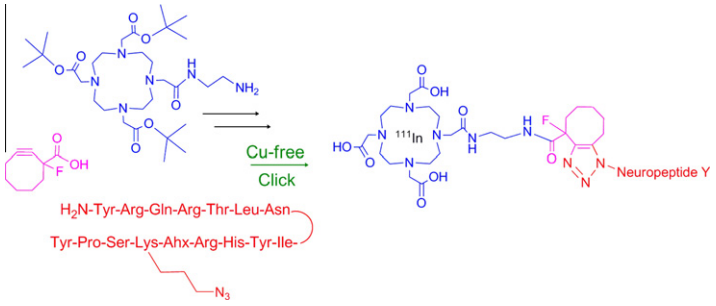

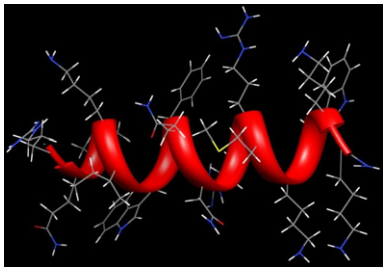

We report the synthesis, the conformational study by using CD spectroscopy and the antifungal assays of penetratin analogues. These peptides displayed a significant antifungal activity against *Candida albicans* and *Cryptococcus neoformans*.

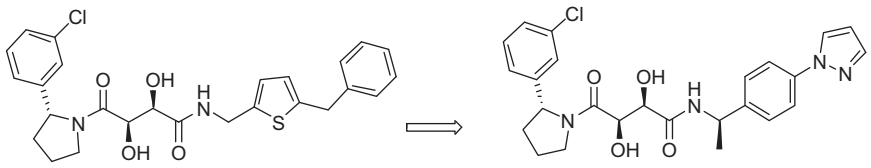

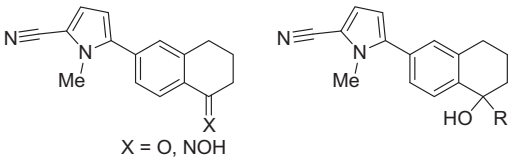

Progesterone receptor antagonists with low nanomolar in vitro potency are reported.

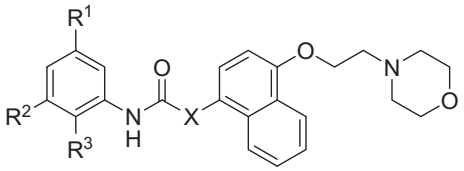

The design and synthesis of novel α-ketoamide based p38 inhibitors is reported.

Two distinct families of small molecules were discovered as novel selective α7 nicotinic acetylcholine receptor (nAChR) antagonists by pharmacophore-based virtual screening. These antagonists exhibited good brain penetration and neuroprotection in a mouse seizure-like behavior model induced by the nerve agent diisopropylfluorophosphate (DFP).

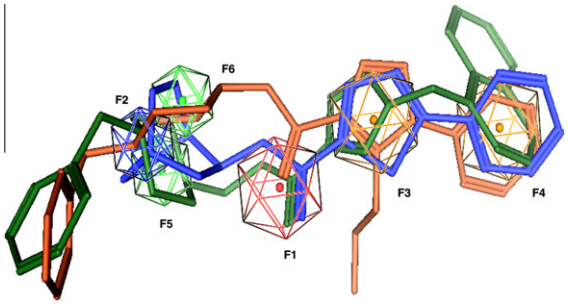

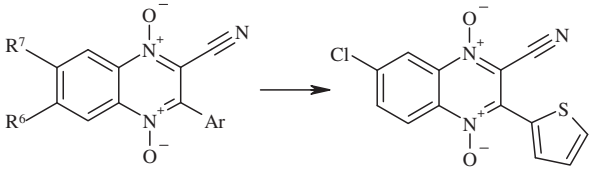

21, IC_{50}=7.1 μM
(Nfx, IC_{50}=7.7 μM)

In vitro anti-*Trypanosoma cruzi* activity and QSAR studies of 3-arylquinoxaline-2-carbonitrile di-*N*-oxides is reported, emerging as new anti-trypanosomal agents. In addition, a rational guide for the proposal of new candidate structures is achieved.

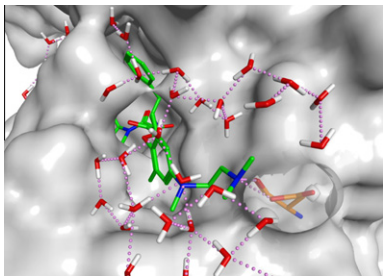

Attachments of 2-aminoethylamino substituents to an allophenylnorstatine-containing plasmepsin inhibitor enhanced both plasmepsin inhibitory and antimalarial activities.

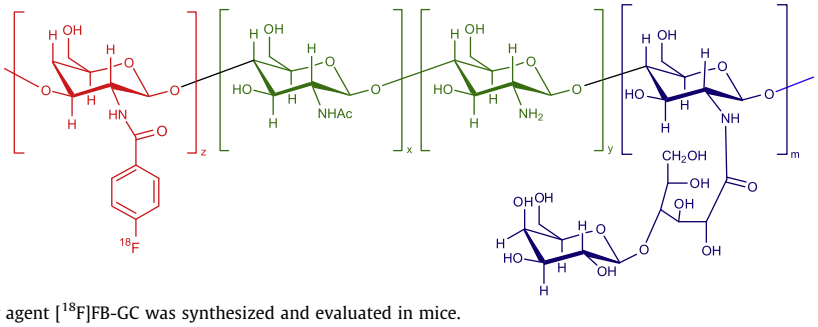

Chitosan based novel ASGP imaging agent [^{18}F]FB-GC was synthesized and evaluated in mice.

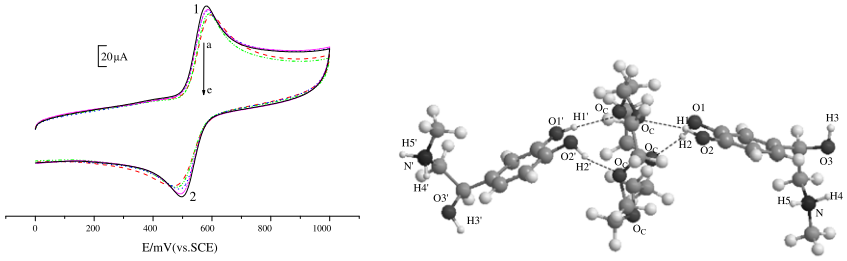

Phosphoramidate ProTides of 2′-C-Me-6-MeOG are up to 500-fold more potent versus HCV than the 2′-C-MeG parent, being active at nanomolar levels. The lead has entered phase 1 clinical trials for HCV.

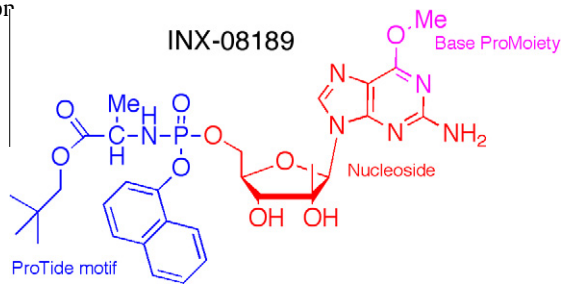

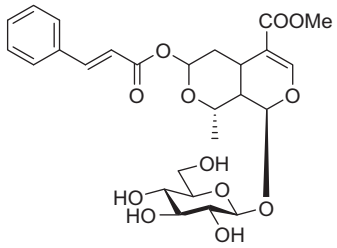

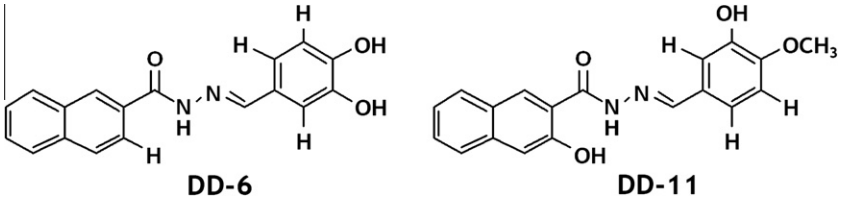

The synthesis of the potent dynamin GTPase inhibitors (IC_{50} = 5.1 μM for DD-6; 3.6 μM for DD-11) is reported.

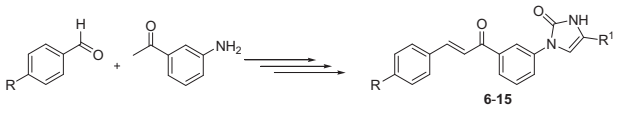

6: R = 4-OH-3-OMe; R^1 = Phenyl
7: R = 4-OH-3-OMe; R^1 = 4 -methoxy phenyl
8: R = 4-OH-3-OMe; R^1 = 4 -chloro phenyl
9: R = 3-OH; R^1 = phenyl
10: R = 3-OH; R^1 = 4 -chloro phenyl
11: R = 3,4,5-(MeO)3; R^1 = phenyl
12: R = 3,4,5-(MeO)3; R^1 = 4 -methoxy phenyl
13: R = 3,4,5-(MeO)3; R^1 = 3,4,5 -trimethoxy phenyl
14: R = 3,4,5-(MeO)3; R^1 = 4 chloro phenyl
15: R = 3-OH; R^1 = naphthyl

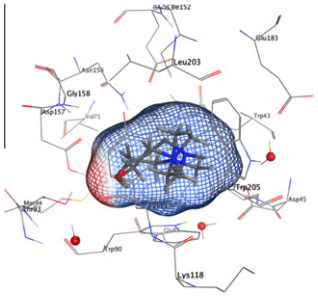

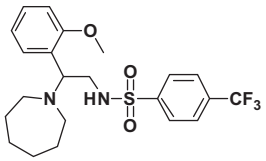

IC_{50} 37 nM

A series of novel GlyT1 inhibitors is described.

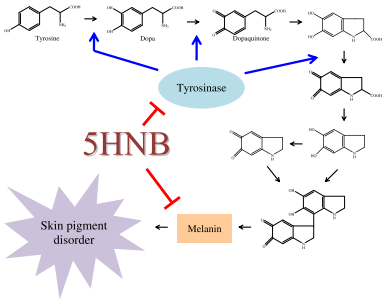

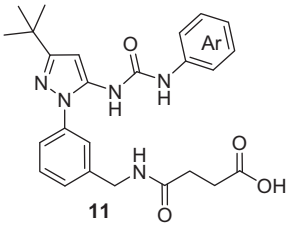

11

The development of potent and selective p38 inhibitor **11** is reported.

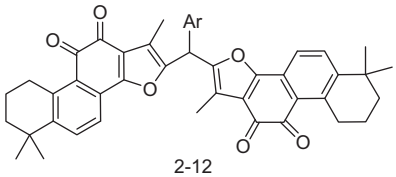

2-12

Vasodilation activity in vitro of them was valuated on the contractile response of vascular thoracic aorta smooth muscle from Wistar rats for the first time. Most of them exhibited a concentration-dependent inhibition of the contractile response of norepinephrine.

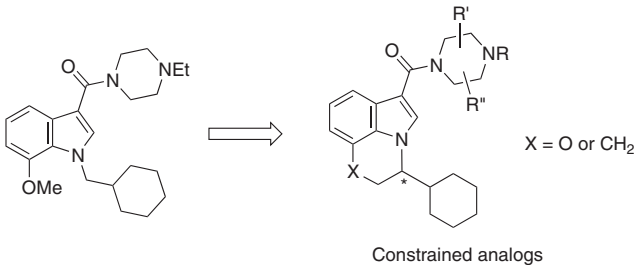

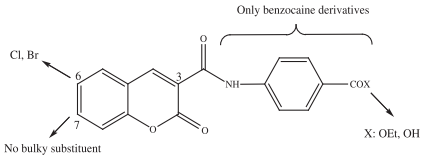

A novel class of 20 N-substituted-3-carboxamido-coumarin derivatives were prepared and evaluated for their selective anti-*Helicobacter pylori* activity against several isolates of clinical strains, including five metronidazole resistant ones. Furthermore, a cytotoxic screening was carried out on the most active derivatives.

Phytochemical investigation resulted in isolation of three new lupane-triterpene glycosides acankoreosides M–O (**1**, **2** and **8**) from the leaves of *Acanthopanax koreanum* (Araliaceae). Compounds **4**, **5**, **7**, and **11** (5, 25, and 100 μM) significantly increased IFN-γ and IL-2 release in spleen cells.

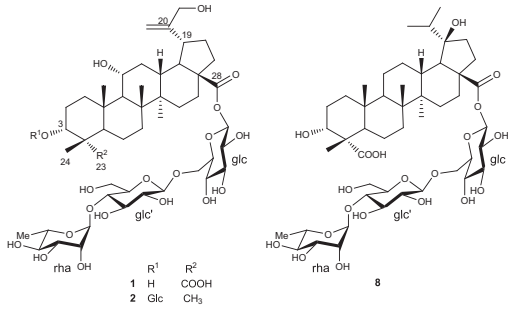

A series of aminomethylpyrazoles were prepared and evaluated using cell-based Smoothened β-lactamase reporter assay and Smoothened binding assay. Potent Smoothened antagonists **10k** and **10l** were found to inhibit hair growth in vivo in the C3H/HeN mouse hair growth model. The more selective compound **10l** was tested negative in the 3T3 NRU assay, indicating a low risk for causing photo-irritation and was efficacious using the C3H/HeN mouse hair growth model although it was slightly less efficacious than that of the reference compound eflornithine (**7**).

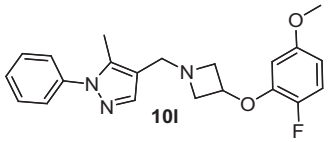

SMOTT, IC_{50} = 8.27 nM
SMOTT, IC_{50} = 124 nM
MED = 3% C3H/HeN mouse

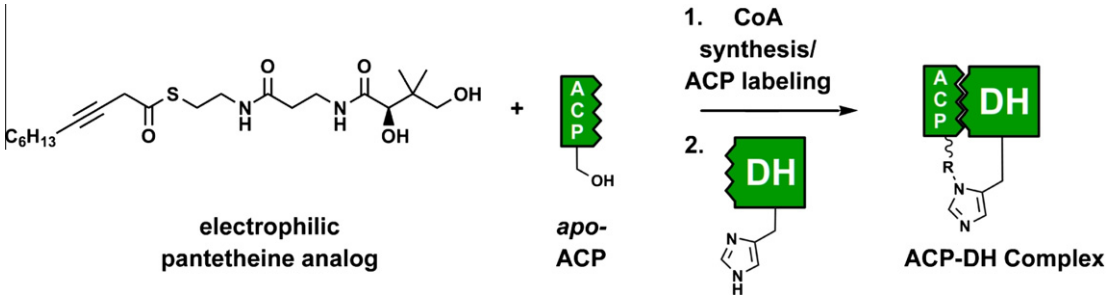

A chemoenzymatic method for the crosslinking of protein partners of the fatty acid biosynthetic pathway is detailed.

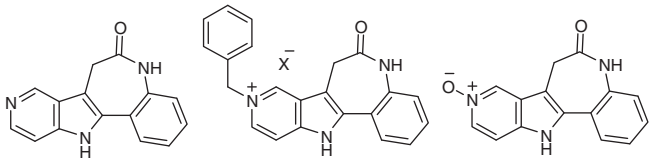

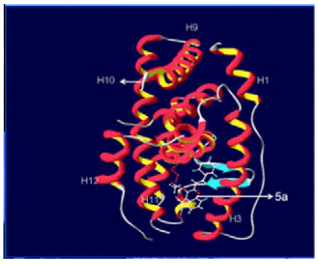

Three dimensional structure of ER β docked with compound **5a** using Maestro.Beta sheet has been shown in blue color and compound has been shown as ball and stick model.

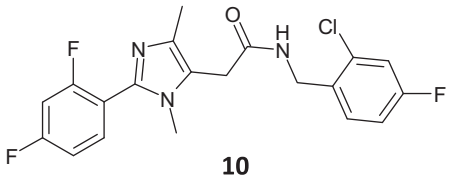

10

$hP2X_7$ pIC_{50} 7.4

OTHER CONTENTS

*Corresponding author
+ Supplementary data available via ScienceDirect
This article does not appear in the printed issue, it is available in the online version of this issue.

COVER

Overlay of high resolution co-crystal structures of *R*-**22**-ADP (cyan) and **1**-ADP (green) bound in an allosteric binding site of the mitotic kinesin KSP. [Roecker, A. J.; Coleman, P. J.; Mercer, S. P.; Schreier, J. D.; Buser, C. A.; Walsh, E. S.; Hamilton, K.; Lobell, R. B.; Tao, W.; Diehl, R. E.; South, V. J.; Davide, J. P.; Kohl, N. E.; Yan, Y.; Kuo, L. C.; Li, C.; Fernandez-Metzler, C.; Mahan, E. A.; Prueksaritanont, T.; Hartman, G. D. *Bioorg. Med. Chem. Lett.* **2007**, *17*, 5677.]

Indexed/Abstracted in: Beilstein, Biochemistry & Biophysics Citation Index, CANCERLIT, Chemical Abstracts, Chemistry Citation Index, Current Awareness in Biological Sciences/BIOBASE, Current Contents: Life Sciences, EMBASE/Excerpta Medica, MEDLINE, PASCAL, Research Alert, Science Citation Index, SciSearch, TOXFILE. Also covered in the abstract and citation database SCOPUS®. Full text available on ScienceDirect®

ELSEVIER

ISSN 0960-894X